

# NEXTCALIBUR - A four-fermion generator for electron-positron collisions

**F. A. Berends**

Instituut Lorentz, University of Leiden, P. O. Box 9506,  
2300 RA Leiden, The Netherlands

**C. G. Papadopoulos**

Institute of Nuclear Physics, NCSR 'Democritos',  
15310 Athens, Greece

and

**R. Pittau**

Dipartimento di Fisica Teorica, Università di Torino, Italy  
INFN, Sezione di Torino, Italy

October 30, 2018

## Abstract

A fully massive Monte Carlo program to compute all four-fermion processes in  $e^+e^-$  collisions, including Higgs boson production, is presented. Leading higher order effects are discussed and included.

Pacs: 11.15.-q, 13.10.+q, 13.38.-b, 13.40.-f, 14.70.-e

# PROGRAM SUMMARY

*Title of program:* NEXTCALIBUR.

*Program obtainable from:* R. Pittau, Dipartimento di Fisica Teorica, Università di Torino, Via Giuria 1, I-10125 Torino-Italy.

*Licensing provisions:* none.

*Computer for which the program is designed and others on which it has been tested:* DIGITAL-ALPHA (double and quadruple precision) and HP (double precision only).

*Operating system under which the program has been tested:* UNIX.

*Programming language used:* FORTRAN 90.

*Memory required:* about 500kbytes.

*number of bits per word:* 32.

*Subprograms used:* none.

*Number of lines in distributed program:* 10274.

*Keywords:* decaying vector-boson production, all massive four-fermion processes, electroweak background, initial state  $p_t$  dependent QED radiation, recursive Dyson-Schwinger equations, multi-channel Monte Carlo approach.

## *Nature of physical problem*

Four-fermion production is and will be investigated at  $e^+e^-$  colliders in a wide range of energies. Fermion masses have to be included when studying Higgs boson production and processes with forward scattered electrons. A Monte Carlo program being able to take into account both signal and background electroweak diagrams for four-fermion processes, without neglecting fermion masses, is therefore required. Higher order effects, such as the QED radiation evaluated at the proper scale, have also to be included, together

with the possibility of generating photons with a non vanishing  $p_t$  spectrum. For  $t$ -channel dominated processes, the correct running of  $\alpha_{EM}$  must be implemented.

#### *Method of solution*

An event generator is the most suitable choice for a program to be able to deal with the above physical problems. For the matrix element evaluation, recursive Dyson-Schwinger equations that express the  $n$ -point Green's functions in terms of the  $1-, 2-, \dots, (n - 1)$ -point functions are used. The Monte Carlo integration is performed by using an efficient self-optimizing multi-channel approach.

*Typical running time:* about 250 weighted events per second, in double precision on DIGITAL-ALPHA/21164 DS20 (500MHz), depending on the chosen physical process.

*Unusual features of the program:* by changing compilation procedure, the program can run both in double and quadruple precision.

## LONG WRITE-UP

### 1 Introduction

Electron-positron collisions have provided an ideal testing ground for the Standard Model. In recent years LEP2 has been instrumental in this. Future colliders may take over this role. At these high energies, final states will be produced containing unstable particles, like a single  $W$ -boson, a Higgs boson or pairs of vector bosons. The net result of this will be a four-fermion final state. It is then not surprising that event generators producing four fermions are in demand. The situation at the start of LEP2 has been described, amongst others, in the 1996 Yellow Report [1] and the present status in the 2000 LEP2 Yellow Report [2].

It has been our aim to provide an event generator, which can produce all possible electroweak four-fermion final states in all possible configurations. Moreover, its accuracy should match the experimental requirements as much as is feasible.

In the early LEP2 days an event generator like EXCALIBUR [3] fulfilled this purpose to a certain extent by producing efficiently all possible massless four-fermion final states. At present, the above aim can only be strived for by

- including fermion masses,
- improving the treatment of QED radiation,
- taking into account scale-dependent corrections and higher order contributions related to unstable particles.

In the first place, fermion masses are needed both for a description of all kinematical regions (e.g. forward scattering) and for the inclusion of Higgs particles.

In the second place, the accuracy should be improved by extending the treatment of QED initial state radiation in two ways. A  $p_t$  effect of emitted photons should be generated and a realistic scale for  $t$ -channel dominated processes should be built in.

Thirdly, the accuracy of the generator can also be increased when large fermion-loop effects on vector boson propagators are taken into account.

The incorporation of these three effects into one event generator led to a completely new program, NEXTCALIBUR. It is the purpose of this paper to describe the program and the built-in physics treatments. Section 2 refers to the new recursive matrix element calculation, section 3 summarizes the phase space generation, whereas the following two sections describe the above mentioned accuracy improving physics effects. Then, sections 6-9 are devoted to the actual program, i.e. its structure, compiling instructions, input and test run output. Finally, two appendices clarify the multiperipheral phase space generation and the adopted fermion-loop scheme.

For those readers, who are interested in the specific physics results of NEXTCALIBUR and some comparisons to other evaluations we refer to ref. [4].

## 2 The Matrix Element evaluation

The algorithm for the computation of the matrix element is based on the Dyson-Schwinger equations, a set of recursive equations that express the  $n$ -point Green's functions in terms of the  $1-$ ,  $2-$ ,  $\dots$ ,  $(n-1)-$ point functions.

For a detailed presentation of the algorithm as well as its `FORTTRAN` implementation, `HELAC`, we refer to ref. [5]. Here we would like to summarize the main advantages of it:

1. Scattering amplitudes involving any Standard Model interaction can be treated, notably the full Higgs sector.
2. Masses of particles are fully considered.
3. Both unitary and Feynman gauges are fully implemented.
4. Quadruple as well as arbitrary precision arithmetic is available, in order to study special kinematical configurations.

One important point we would like to underline here is that the algorithm makes use of the chiral representation for fermions and therefore it is more or less equivalent in efficiency to the method used by `EXCALIBUR` [3] for massless fermions.

Because of its modular structure, the algorithm can easily incorporate higher order contributions to the scattering amplitude, and in fact several such contributions have been included. The user has to specify the corresponding flags and input parameters, as described in section 8, in order to study these higher order effects.

### 3 The integration strategy

The integration strategy in `NEXTCALIBUR` is the same adopted in ref. [3], namely a multi-channel self-optimizing [6] approach.

All possible peaking structures of the integrand are taken into account by the 19 different kinematical channels (plus momenta permutations) in fig. 1. The conventions to read off the peaking structure are as follows. Fermionic lines have an arrow, wavy lines represent photons while dashed lines are massive gauge bosons. Solid lines connect topological equivalent points: a  $t$ -channel solid line means isotropic angular distribution between the connected fermions, while an  $s$ -channel line only gives rise to an  $s$  dependent behaviour, without affecting the peaking structure.

The difference with the channels of ref. [3] is that now all fermions are taken to be massive.

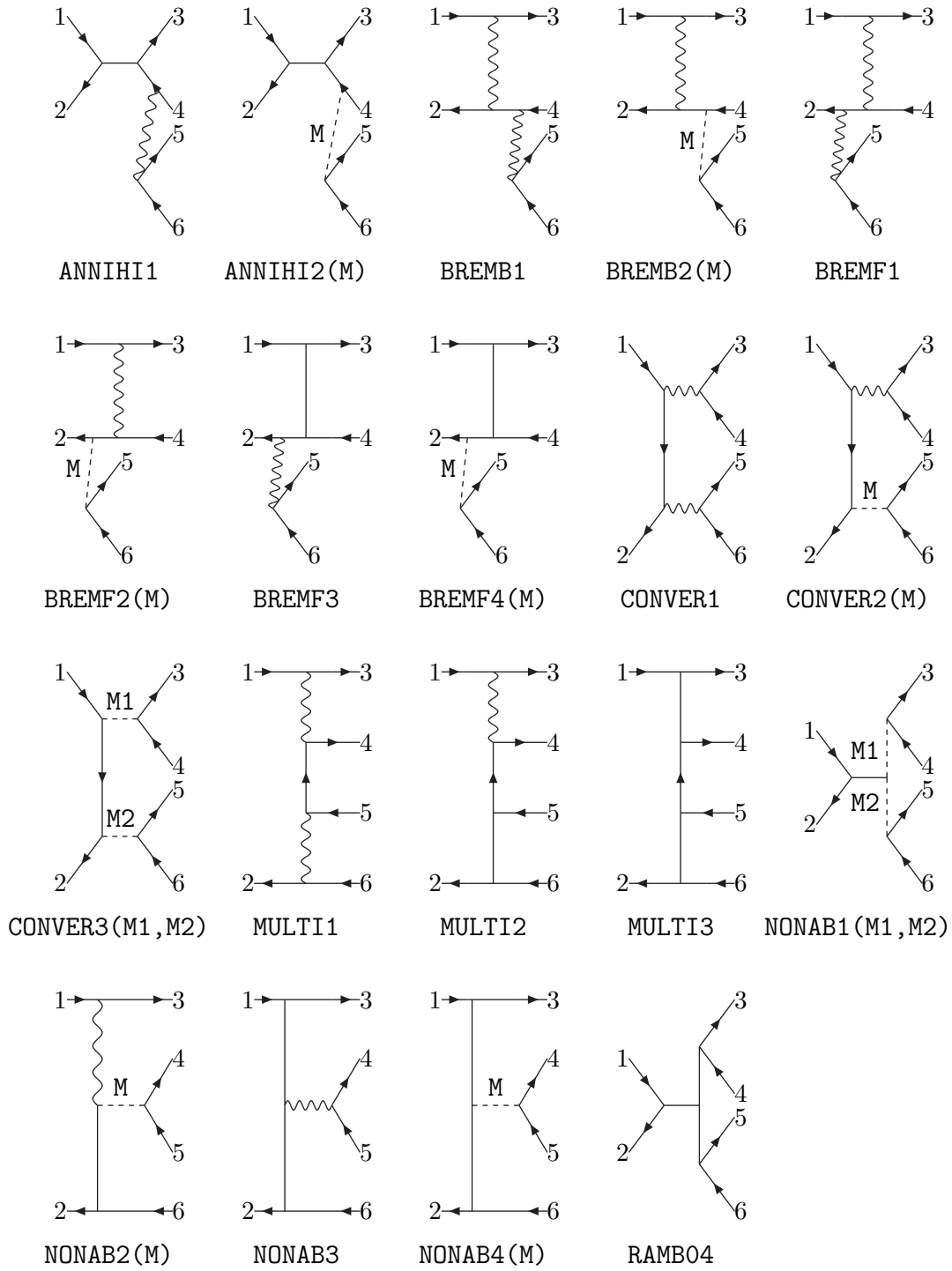


Figure 1: kinematical diagrams in NEXTCALIBUR.

Furthermore, the leading kinematical structures for Higgs boson production have been added. They are represented by the channels `NONAB1(M1,M2)` and `NONAB4(M)`, where the masses can now also be the Higgs mass.

Generally speaking, the modification from the old massless to the new massive channels required only trivial changes. An exception is represented by the channel `MULTI1`, for which we list, in appendix A, the complete generation algorithm.

A last remark is in order. When dealing with final state electrons, strong numerical cancellations occur, that may degrade the accuracy of the phase space generation. In order to overcome this problem a number of tricks are applied all over the places in `NEXTCALIBUR`, all derived from the basic identity

$$q_0 - |\vec{q}| = \frac{m_e^2}{(q_0 + |\vec{q}|)}, \quad \text{where} \quad q^2 = m_e^2, \quad q = (q_0, \vec{q}). \quad (1)$$

## 4 Treatment of the QED radiation

In `NEXTCALIBUR` QED radiation is implemented via the Structure Function formalism, namely by convoluting the Born cross section together with QED Initial State Radiators [7]. Two ISR photons are explicitly generated, by using  $p_t$  dependent Structure Functions [8], derived, at the first leading logarithmic order, for small values of  $p_t$  [9]. Our starting point is the convolution

$$\sigma(s) = \int dx_1 dx_2 dc_1 dc_2 \frac{1}{2\pi} \int_0^{2\pi} d\phi_1 \frac{1}{2\pi} \int_0^{2\pi} d\phi_2 \Phi(x_1, c_1) \Phi(x_2, c_2) \sigma_0(\hat{s}), \quad (2)$$

where  $\sigma_0$  is the Born four-fermion cross section,  $\hat{s}$  the reduced center of mass energy of the event, after photon emission,  $c_{1,2}$  and  $\phi_{1,2}$  the cosines of the directions (in the laboratory frame) and the azimuthal angles of the two emitted photons with respect to the incoming particles. Finally, the Structure Functions are given by

$$\begin{aligned} \Phi(x, c, q^2) = & \\ & \frac{\exp\left\{\frac{1}{2}\beta\left(\frac{3}{4} - \gamma_E\right)\right\}}{\Gamma\left(1 + \frac{1}{2}\beta\right)} \frac{\alpha}{\pi} (1-x)^{\frac{\beta}{2}-1} \left( \frac{1}{1-c + 2\frac{m_e^2}{q^2}} - 2\frac{m_e^2}{q^2} \frac{1}{(1-c + 2\frac{m_e^2}{q^2})^2} \right) \\ & - \frac{\alpha}{2\pi} (1+x) \left( \frac{1}{1-c + 2\frac{m_e^2}{q^2}} + \frac{1-x}{1+x} \cdot \frac{1}{2} - 4\frac{m_e^2}{q^2} \frac{1}{(1+x)(1-c + 2\frac{m_e^2}{q^2})^2} \right) \end{aligned}$$

$$\begin{aligned}
& + \frac{\beta}{8} \frac{\alpha}{2\pi} \left[ -4(1+x) \ln(1-x) + 3(1+x) \ln x - 4 \frac{\ln(x)}{1-x} - 5 - x \right] \\
& \times \left( \frac{1}{1-c + 2\frac{m_e^2}{q^2}} + \frac{1-x}{1+x} \cdot \frac{1}{2} - 4 \frac{m_e^2}{q^2} \frac{1}{(1+x)(1-c + 2\frac{m_e^2}{q^2})^2} \right), \quad (3)
\end{aligned}$$

with

$$\beta = 2 \frac{\alpha}{\pi} \left( \ln\left(\frac{q^2}{m_e^2}\right) - 1 \right). \quad (4)$$

The above formula can be obtained by *unfolding* the strictly collinear Structure Functions, with the replacement

$$\ln\left(\frac{q^2}{m_e^2}\right) - 1 \rightarrow \frac{1}{1-c + 2\frac{m_e^2}{q^2}} - 2 \frac{m_e^2}{q^2} \frac{1}{(1-c + 2\frac{m_e^2}{q^2})^2} \quad (5)$$

for the soft part, and

$$\ln\left(\frac{q^2}{m_e^2}\right) - 1 \rightarrow \frac{1}{1-c + 2\frac{m_e^2}{q^2}} + \frac{1-x}{1+x} \cdot \frac{1}{2} - 4 \frac{m_e^2}{q^2} \frac{1}{(1+x)(1-c + 2\frac{m_e^2}{q^2})^2} \quad (6)$$

for the hard contributions<sup>1</sup>. With this choice, the whole expression gets proportional to  $\ln(\frac{q^2}{m_e^2}) - 1$ , after integrating over  $c$ , as it should be. The inclusive QED result is therefore recovered and, at the same time, the pattern of the photon radiation is exact for small values of  $p_t$ .

The generation algorithm is as follows. The initial state electrons, before radiating, have momenta given by

$$p_1 = (E, \beta E, 0, 0), \quad p_2 = (E, -\beta E, 0, 0), \quad E = \frac{\sqrt{s}}{2}, \quad \beta = \sqrt{1 - \frac{m_e^2}{E^2}}. \quad (7)$$

Once  $c_{1,2}$  are generated, together with the energy fractions  $x_{1,2}$  and the azimuthal angles  $\phi_{1,2}$ , the momenta of the two ISR photons are completely determined

$$\begin{aligned}
q_1 &= E(1-x_1)(1, c_1, s_1 \cos \phi_1, s_1 \sin \phi_1), \\
q_2 &= E(1-x_2)(1, -c_2, s_2 \cos \phi_2, s_2 \sin \phi_2), \quad s_i = \sqrt{1 - c_i^2}, \quad (8)
\end{aligned}$$

---

<sup>1</sup>Note that the replacement of eq. (6) is also performed in the higher order terms of eq. (3).



and the invariant mass, after ISR, is given by

$$\begin{aligned}
\hat{s} &= \ell^2 \equiv (\ell_1 + \ell_2)^2 \\
&= s \left\{ x_1 x_2 + \frac{(1-x_1)(1-x_2)}{2} [c_1 c_2 - 1 - s_1 s_2 \cos(\phi_1 - \phi_2)] \right\}, \\
\ell_1 &\equiv p_1 - q_1, \quad \ell_2 \equiv p_2 - q_2.
\end{aligned} \tag{9}$$

We then generate four-fermion events in the center-of-mass frame of  $\ell$ , where the new  $x$  direction *after* ISR is determined by the spatial part of the four-vector obtained by boosting  $\ell_1$  in the center-of-mass frame. All generated four-fermion momenta are subsequently boosted back to the Laboratory frame.

In **NEXTCALIBUR** there is also the possibility of generating strictly collinear radiation. In this case the relevant formulae are

$$\begin{aligned}
\sigma(s) &= \int dx_1 dx_2 \Phi(x_1) \Phi(x_2) \sigma_0(\hat{s}), \\
\Phi(x, q^2) &= \frac{\exp\left\{\frac{1}{2}\beta\left(\frac{3}{4} - \gamma_E\right)\right\}}{\Gamma\left(1 + \frac{1}{2}\beta\right)} \frac{\beta}{2} (1-x)^{\frac{\beta}{2}-1} - \frac{\beta}{4} (1+x) \\
&\quad + \frac{1}{32} \beta^2 \left[ -4(1+x) \ln(1-x) + 3(1+x) \ln x - 4 \frac{\ln(x)}{1-x} - 5 - x \right],
\end{aligned} \tag{10}$$

with  $\beta$  defined in eq. (4). In order to allow particular QED studies, the generation of photons in **NEXTCALIBUR** has been kept independent for each of the two incoming legs. This implies the possibility of two different scales  $q_-^2$  and  $q_+^2$  for the electron and positron leg respectively. Mixed situations are also possible, in which one leg produces a collinear photon, while the other generates a photon with  $p_t$ . This can be controlled at the level of the input file, as explained in the next sections.

A second issue, relevant when studying QED radiation, is the choice of the  $q^2$  to be inserted in the Structure Functions of eq. (3) and/or eq. (10). The choice  $q^2 \sim s$  is proven to reproduce accurately the inclusive four-fermion cross sections, at least for  $s$ -channel dominated processes. For  $t$ -channel dominated processes a different choice is more adequate, as studies of certain processes have shown. When an exact first order QED radiative correction calculation exists for a  $t$ -channel dominated process, then the result can

be compared to a Structure Function calculation with a  $q^2$  scale related to the virtuality of the exchanged  $t$ -channel photon. With such a  $q^2$  value the two kinds of calculations agree for small angle Bhabha scattering [10] and multi-peripheral two-photon processes [11], where the exact calculation already exists for some time [12]. When no exact first order QED correction calculation is available, the first order soft correction may also serve as a guideline to determine  $q^2$  [11, 13]. In NEXTCALIBUR, the choice of the scale is performed automatically, event by event, according to the selected final state, as shown in Table 1.

| Final State         | $q_-^2$       | $q_+^2$       |
|---------------------|---------------|---------------|
| No $e^\pm$          | $s$           | $s$           |
| 1 $e^-$             | $ t_- $       | $s$           |
| 1 $e^+$             | $s$           | $ t_+ $       |
| 1 $e^-$ and 1 $e^+$ | $ t_- $       | $ t_+ $       |
| 2 $e^-$ and 2 $e^+$ | $\min( t_- )$ | $\min( t_+ )$ |

Table 1: The choice of the QED scale in NEXTCALIBUR.  $q_\pm^2$  are the scales of the incoming  $e^\pm$  while  $t_\pm$  represent the  $t$ -channel invariants obtained by combining initial and final state  $e^\pm$  momenta. When two combinations are possible, as in the last entry of the table, that one with the minimum value of  $|t|$  is chosen, event by event.

When using Structure Functions with a  $t$ -channel scale, one faces inefficiencies in the event generation. To illustrate the problem, we start from a simple model, namely a single collinear photon generated with a distribution given by the leading behaviour of eq. (10), namely

$$\Phi(x) \sim \frac{1}{(1-x)^{(1-z)}}, \quad z = \frac{\alpha}{\pi} \left( \ln\left(\frac{|t|}{m_e^2}\right) - 1 \right). \quad (11)$$

The relevant integral is

$$I = \int_0^1 dx \int d(PS)_4 \Phi(x) |M(t)|^2, \quad (12)$$

where  $d(PS)_4$  is the four-body phase-space integration element and  $|M(t)|^2$  the  $t$  dependent four-fermion Born matrix element squared. The usual way to

cure the peaking behaviour of  $\Phi(x)$  would be performing a change of variable

$$(1-x) = \rho^{\frac{1}{z_g}}, \quad 0 < \rho < 1 \text{ uniformly} \quad (13)$$

so that

$$I = \int_0^1 d\rho \int d(P\mathcal{S})_4 \left( -\frac{1}{z_g} \right) (1-x)^{(z-z_g)} |M(t)|^2, \quad (14)$$

and choosing  $z_g = z$ , namely

$$z_g = \frac{\alpha}{\pi} \left( \ln\left(\frac{t_g}{m_e^2}\right) - 1 \right) \quad (15)$$

with  $t_g = |t|$ .

The problem here is that, with our QED model,  $x$  has to be generated, through eqs. (13) and (15), *before* knowing  $t$ . The latter is in fact related to the subsequent generation of the four-fermion event. An initial  $t_g$  must therefore be employed, that is not directly related to the *true* generated  $t$ . Therefore, event by event, the numerical value of the term

$$(1-x)^{(z-z_g)} = (1-x)^{\frac{\alpha}{\pi} \ln \frac{|t|}{t_g}} \quad (16)$$

in eq. (14) may vary considerably, leading to Monte Carlo inefficiencies.

Our strategy is as follows. Since eq. (14) does not depend on  $t_g$ , we are free to integrate over an extra uniform variable  $0 < \rho_0 < 1$ , that we also use to generate  $t_g$  distributed as  $1/t_g$  between a minimum ( $t_g^-$ ) and a maximum value ( $t_g^+ = s$ )

$$t_g = t_g^- \left( \frac{t_g^+}{t_g^-} \right)^{\rho_0}. \quad (17)$$

Our integral then becomes

$$I = \int_0^1 d\rho_0 \int_0^1 d\rho \int d(P\mathcal{S})_4 \left( -\frac{1}{z_g} \right) (1-x)^{(z-z_g)} |M(t)|^2, \quad (18)$$

with  $z_g$  and  $t_g$  given in eqs. (15) and (17). We have chosen  $t_g$  distributed as  $1/t_g$  because this is the expected behaviour of the *true*  $t$  coming from

$|M(t)|^2$ , when small  $t$ -channel scales dominate. However, this alone does not yet prevent a blowing of the term in eq. (15) for a few events. We therefore split the integration range of  $\rho_0$  into  $n$  equidistant bins, introduce a set of weights  $\alpha_i$ , normalized such that  $\sum_{i=1}^n \alpha_i = 1$ , and rewrite

$$\begin{aligned}
I &= n \sum_{i=1}^n I_i, \\
I_i &= \int_{\rho_{0i}^-}^{\rho_{0i}^+} d\rho_0 \int_0^1 d\rho \int d(P\mathcal{S})_4 \alpha_i \left(-\frac{1}{z_g}\right) (1-x)^{(z-z_g)} |M(t)|^2, \\
\rho_{0i}^- &= \frac{i-1}{n}, \quad \rho_{0i}^+ = \frac{i}{n}.
\end{aligned} \tag{19}$$

Since  $\rho_{0i}^- < \rho_0 < \rho_{0i}^+$  corresponds to the  $i^{\text{th}}$  generation interval

$$t_{gi}^- < t_g < t_{gi}^+, \quad t_{gi}^\pm = t_g^- \left(\frac{t_g^+}{t_g^-}\right)^{\rho_{0i}^\pm}, \tag{20}$$

eq. (19) allows to weight differently events produced in different intervals. Notice that the set of weights  $\{\alpha_i\}$  can depend on  $t$ . A suitable choice is

$$\alpha_i \equiv \alpha_i(|t_j|^-) = \frac{(1-x)^{\frac{\alpha}{\pi} \ln \frac{t_{gj}^-}{|t_j|^-}}}{\sum_i (1-x)^{\frac{\alpha}{\pi} \ln \frac{t_{gj}^-}{|t_j|^-}}}. \tag{21}$$

The meaning of  $|t_j|^-$  in the above formula is as follows. Once  $t_g$  is produced as described, the four-fermion event can be generated with a given value of  $t$  (the *true t*). The variable  $|t|$  can then be binned as done for  $t_g$  in eq. (20) and, if  $t_{gj}^- < |t| < t_{gj}^+$ ,  $|t_j|^- = t_{gj}$ . Then, even by event, the set  $\{\alpha_i\}$  changes, compensating the term in eq. (16) and improving the generation efficiency.

Summarizing, the Monte Carlo implementation of the technique is

- 1) divide the interval  $[0,1]$  in  $n$  equidistant bins;
- 2) generate  $\rho_0$  uniformly in  $[0,1]$   
 $\Rightarrow i$  and  $t_{gi}^-$  are known;
- 3) generate ISR and the four-fermion event  
 $\Rightarrow$  the event weight  $w$ , the variable  $t$ ,  $j$  and  $|t_j|^-$  are known;

$$4) \quad w \rightarrow w \cdot n \cdot \alpha_i(|t_j|^-).$$

The algorithm works unchanged when both initial state particles radiate, and when photons are generated with a non vanishing  $p_t$ . In this latter case, eq. (11) is replaced by

$$\Phi(x, c) \sim \frac{1}{(1-x)^{(1-z)}} \frac{1}{1-c + 2\frac{m_e^2}{|t|}}. \quad (22)$$

The generation of  $x$  is as described previously. In addition,  $c$  is generated with distribution

$$\frac{1}{1-c + 2\frac{m_e^2}{t_g}},$$

and the weights  $\alpha_i$  modified accordingly, in order to compensate the term

$$\frac{1-c + 2\frac{m_e^2}{t_g}}{1-c + 2\frac{m_e^2}{|t|}} \quad (23)$$

appearing in the event weight.

A last comment is in order on our QED modelling. By using  $q^2 = |t|$  in the Structure Functions, a few events are produced with very low values of  $\ln(|t|/m_e^2)$ , when  $|t| \sim m_e^2$ . This means that logarithms are no longer leading, breaking down the Structure Function approach. Constant terms should in principle be included. On the other hand, low values of  $\ln(|t|/m_e^2)$  imply  $\Phi(x) \sim \delta(1-x)$ , resulting in a suppression of the QED radiation, as confirmed by direct calculations [10, 12]. Notice that even implementing the exact form of the Structure Functions, also valid for  $|t| < m_e^2$  [14], only includes the factorizable part of the missing constants and not all of them. In the present version of NEXTCALIBUR we follow a different strategy and introduce a minimum  $|t|_{min}$ , such that, if  $|t| < |t|_{min}$ , the ISR logarithm is always evaluated at  $q^2 = |t|_{min}$ <sup>2</sup>. With  $|t|_{min} = 100 m_e^2$ , the minimum value of the logarithm still gives physical results, but is small enough to reproduce the discussed radiation suppression. We checked the insensitivity of our results to the choice of  $|t|_{min}$  in the range  $50 m_e^2 < |t|_{min} < 200 m_e^2$ .

---

<sup>2</sup>We consequently put  $t_g^- = |t|_{min}$  in eq. (17).

## 5 The running of $\alpha_{EM}$

When studying high energy processes, part of the higher order corrections can be reabsorbed in the Born approximation by using the so-called  $G_F$  scheme. In such a scheme  $G_F$ ,  $M_Z$  and  $M_W$  are input parameters, while the weak mixing angle and  $\alpha_{EM}$  are derived quantities:

$$\begin{aligned} s_W^2 &= 1 - M_W^2/M_Z^2, \\ \alpha_{EM} &= \sqrt{2} \frac{G_F M_W^2 s_W^2}{\pi}. \end{aligned} \quad (24)$$

In the presence of low  $t$ -channel scales such an approach fails, since the choice  $\alpha(t \sim 0) \sim 1/137$  is certainly more appropriate for certain sets of diagrams and/or kinematical regions. The question is therefore how to include consistently the running of  $\alpha_{EM}$  in four-fermion processes with one or more electrons in the final state.

An exact and field-theoretically consistent solution to this problem is represented by the Fermion-Loop approach of refs. [15]-[17], where the whole set of fermion one-loop corrections is taken into account by computing running couplings  $g(s)$  and  $e(s)$  and re-summed bosonic propagators.

In the presence of the  $WW\gamma$  vertex, also loop mediated vertices are required to preserve gauge invariance. On the contrary, when the  $WW\gamma$  coupling is absent, the neutral gauge boson vertices, induced by the fermion loop contributions, are separately gauge invariant [16].

Since the exact expression of the loop-induced vertex functions is rather cumbersome, we follow a simplified approach (Modified Fermion-Loop approach) by neglecting the separately gauge invariant neutral boson vertices and including only the part of the  $WW\gamma$  loop function necessary to preserve the  $U(1)$  gauge invariance. Besides running couplings, we use bosonic propagators

$$\begin{aligned} P_w^{\mu\nu}(s) &= (s - M_W^2(s))^{-1} \left( g_{\mu\nu} - \frac{p_\mu p_\nu}{M_W^2(s)} \right) \\ P_z^{\mu\nu}(s) &= (s - M_Z^2(s))^{-1} \left( g_{\mu\nu} - \frac{p_\mu p_\nu}{M_Z^2(s)} \right), \end{aligned} \quad (25)$$

with running boson masses defined as

$$\begin{aligned}
M_W^2(s) &= \mu_w \frac{g^2(s)}{g^2(\mu_w)} - g^2(s)[T_W(s) - T_W(\mu_w)] \\
M_Z^2(s) &= \mu_z \frac{g^2(s)}{c_\theta^2(s)} \frac{c_\theta^2(\mu_z)}{g^2(\mu_z)} - \frac{g^2(s)}{c_\theta^2(s)} [T_Z(s) - T_Z(\mu_z)]. \quad (26)
\end{aligned}$$

$T_{W,Z}(s)$  are contributions due to the top quark,  $\mu_{w,z}$  the complex poles of the propagators and

$$s_\theta^2(s) = \frac{e^2(s)}{g^2(s)}, \quad c_\theta^2(s) = 1 - s_\theta^2(s).$$

The explicit form of the running functions  $e^2(s)$ ,  $g^2(s)$  and  $T_{W,Z}(s)$  can be found in appendix B, together with more details on our procedure. Here we just mention that, since the leading contributions are in the real part of the running couplings, we replace complex poles by complex masses and only consider the real part of the corrections. This in practice means replacing

$$\begin{aligned}
\mu_{w,z} &\rightarrow M_{W,Z}^2 - i\Gamma_{W,Z}M_{W,Z}, & g^2(\mu_{w,z}) &\rightarrow g^2(M_{W,Z}^2), \\
c_\theta^2(\mu_z) &\rightarrow c_\theta^2(M_Z^2), & T_{W,Z}(\mu_{w,z}) &\rightarrow T_{W,Z}(M_{W,Z}^2), \quad (27)
\end{aligned}$$

in the above formulae. Note that, as for the treatment of the gauge boson widths, this is equivalent to the fixed width scheme [17].

When also the  $WW\gamma$  coupling contributes, we introduce, in addition, the following effective three gauge boson vertex

$$\begin{array}{c}
\begin{array}{c}
p_+ \\
\swarrow \\
W_\nu^+
\end{array} \\
\begin{array}{c}
\gamma_\mu \text{ wavy line} \xrightarrow{p} \bullet \\
\searrow \\
p_- \\
\swarrow \\
W_\rho^-
\end{array}
\end{array} = i e(s) V_{\mu\nu\rho}$$

with  $s = p^2$ ,  $s^+ = p_+^2$ ,  $s^- = p_-^2$  and

$$V_{\mu\nu\rho} = g_{\mu\nu}(p - p_+)_\rho + g_{\nu\rho}(p_+ - p_-)_\mu (1 + \delta_V) + g_{\rho\mu}(p_- - p)_\nu$$

$$\begin{aligned}
& + \frac{(p_+ - p_-)_\mu}{s^- - s^+} \left[ \left( \frac{g(s^-)}{g(s^+)} - 1 \right) p_{+\nu} p_{+\rho} - \left( \frac{g(s^+)}{g(s^-)} - 1 \right) p_{-\nu} p_{-\rho} \right] \\
\delta_V & = \frac{1}{g(s^+)g(s^-)(s^- - s^+)} \left[ g^2(s^+)g^2(s^-) [T_W(s^-) - T_W(s^+)] \right. \\
& \left. + [g(s^+) - g(s^-)] [s^- g(s^+) + s^+ g(s^-)] \right]. \tag{28}
\end{aligned}$$

It is the easy to see that, with the above choice for  $V_{\mu\nu\rho}$ , the  $U(1)$  gauge invariance - namely current conservation - is preserved, even in presence of complex masses and running couplings, also with massive final state fermions.

To preserve  $U(1)$ , one can either compute  $g(s)$  at a fixed scale (for example always at  $s = M_W^2$ ), while keeping only the running of  $e(s)$ , or let all the couplings run at the proper scale. With the first choice the modification of the three gauge boson vertex is kept minimal (but the leading running effects are still included). With the second choice everything runs, but a heavier modification of the Feynman rules is required. Since our approach is an effective one, its quality can be judged only by comparing with the exact calculation of ref. [15]. We found that the second choice gives a better agreement for leptonic single- $W$  final states, while the first one is closer to the exact result in the hadronic case, which is phenomenologically more relevant. Therefore, we adopted this first option as our default implementation in NEXTCALIBUR.

When using NEXTCALIBUR in the described *running coupling mode*,  $U(1)$  gauge invariance is preserved but  $SU(2)$  is, in general, violated. The effects of such a violation are small at LEP2 energies. In fact our method turned out to be numerically equivalent, at  $\sqrt{s} \sim 200$  GeV, to the IFL $_\alpha$  approach of ref. [18]. The authors of ref. [18] divide all Feynman diagrams in gauge invariant sets and use different electromagnetic couplings for each set, therefore preserving  $SU(2) \times U(1)$  gauge invariance. Our method is more suitable in all cases when no easy separation in different classes of Feynman diagrams is possible.

An alternative  $SU(2) \times U(1)$  preserving scheme is represented by the formalism of ref. [19], where extra terms are introduced in the Lagrangian to compensate the self-energies contributions and restore gauge invariance.

A version of NEXTCALIBUR implementing the equations of ref. [19] is currently under development.



## 6 Structure of the program

We shall briefly describe here the general structure of the program. In the `MAIN` of `NEXTCALIBUR` the input file is read and various initializations are performed, for the matrix element evaluation and the phase space generation.

The phase space is initialized by calling `SUBROUTINE SETPRO`, where the kinematical channels for the phase space generation are build up, according to the chosen four-fermion final state. In `SUBROUTINE SETPRO` also the input parameter set has to be specified. The values to be provided are  $G_F$  (`GFERMI`),  $M_Z$  (`ZM`),  $M_W$  (`WM`),  $\Gamma_Z$  (`ZW`),  $\sin^2 \theta_W$  (`SINW2`),  $\alpha_{EM}$  (`ALPHA`), and  $\Gamma_W$  (`WW`). The recommended choice, implemented by default, is the  $G_F$  scheme described in section 5. A value for the Higgs mass (`HM`) has to be specified as well and the corresponding tree level value of  $\Gamma_H$  (`HW`) is computed with the formula

$$\Gamma_H = \frac{\alpha_{EM} M_H}{8M_W^2 \sin^2 \theta_W} (m_\tau^2 + 3m_b^2 + 3m_c^2)$$

$$m_\tau = 1.777 \text{ GeV}, \quad m_c = 0.75 \text{ GeV}, \quad m_b = 2.9 \text{ GeV}. \quad (29)$$

Finally, `SUBROUTINES PHYSICS` and `HELAC_INIT` are called, to initialize the evaluation of the Matrix Element.

The generation of the QED Initial State Radiation is performed in the `MAIN` of the program. The used algorithm has been extensively described in section 4. The number of bins used in eq. (19) to integrate over  $t$ -dependent Structure Functions is set by the variables `nisr10`, `nisr11`, `nisr20` and `nisr21`. All remaining subroutines are devoted either to the matrix element evaluation or to the phase space integration.

Additional cuts, besides those ones specified in the input file, must be implemented directly in `SUBROUTINE CUTS`, where the two commons

```
COMMON/AREA10/PM1(0:4,1:6),PM4(12:65),OMCT1(1:6,3:6)
COMMON/PHOTONS/PM1G(0:4,1:3)
```

contain the fermion four-momenta computed in the Lab frame (`PM1`), the invariant mass squared among all possible particle pairs (`PM4`), the quantities  $1 - \cos \theta_{ij}$  (`OMCT1`) and the momenta of the two ISR photons (`PM1G`). If the event is rejected `LNOT= 1`, and the weight is put to zero.

The conventions for the momenta are as follows:

PM1(0,j) is the energy of the  $j^{th}$  particle  
PM1(1,j) is the x component  
PM1(2,j) is the y component  
PM1(3,j) is the z component  
PM1(4,j) is the four-momentum squared.

Particles number 1 and 2 are the incoming  $e^+$  and  $e^-$ , respectively. The beam is along the x axis and  $e^+$  is along the positive direction.

PM1G(0:4,1) is the four momentum of the photon generated by the incoming  $e^+$ , PM1G(0:4,2) that one coming from the  $e^-$  and PM1G(0:4,3) is the most energetic between the two. PM1G(0:4,j) is different from zero only when ISR is generated with a non-vanishing  $p_t$  distribution.

The event weight is W, the final value of which is computed immediately before the FORTRAN line

```
IF (I.GT.0) CALL INBOOK(1,W,IINIT).
```

The status of the run can be checked with the help of the file `monitor`, in which the output file name and the used Monte Carlo points are printed out every 5000 iterations (with negative values during the warming phase). In the file `backup` the intermediate result is stored every 50000 Monte Carlo points.

## 7 Compiling instructions

NEXTCALIBUR is written in FORTRAN 90. The main program is `nextcalibur.f` and there are five included files, namely

```
declare.h  
declare_dp.h (to run in double precision)  
declare_qp.h (to run in quadruple precision)  
compl_mass.h  
list.h.
```

NEXTCALIBUR can be run both in double and quadruple precision. Double precision is sufficient to run all processes without electrons (or positrons) among the final state particles, or processes with final state electrons (or

positrons) with *at most* one final state electron (or positron) allowed in the zero-angle forward region. To run in double precision, typical compiling instructions are:

```
> cp declare_dp.h > declare.h
> f90 -O nextcalibur.f -o nextcalibur.out
> nextcalibur.out < nextcalibur.in
```

where `nextcalibur.in` is the input file (see next section).

To run processes with more than one final state electron (or positron) allowed in the zero-angle forward region, quadruple precision should be used, instead. A typical example is the process  $e^+e^- \rightarrow e^+e^-\mu^+\mu^-$  *without* any cut. To run in quadruple precision, typical compiling instructions are:

```
> cp declare_qp.h > declare.h
> f90 -O -double_size 128 nextcalibur.f -o nextcalibur.out
> nextcalibur.out < nextcalibur.in
```

The flag `-double_size 128` (that treats double precision real numbers as quadruple precision real numbers) *is essential*.

## 8 Input

In this section we list the meaning of the input parameters to be specified by the user:

PAR(3) (CHARACTER\*2)

Produced fermion with label 3 (to be chosen among 'EL', 'NE', 'MU', 'NM', 'TA', 'NT', 'UQ', 'DQ', 'CQ', 'SQ', 'TQ', 'BQ').

PAR(4) (CHARACTER\*2)

Produced fermion with label 4.

PAR(5) (CHARACTER\*2)

Produced fermion with label 5.

PAR(6) (CHARACTER\*2)

Produced fermion with label 6.

NIPT (INTEGER)

The number of points for the Monte Carlo integration.

NWARM (INTEGER)

Number of points for the warming up of the phase space generation but not used for the actual computation. For processes with zero angle electrons in the final state it is recommended to chose a non zero value (e.g. NWARM=10000).

NOPT (INTEGER)

Number of points for the phase space optimization but also used for the computation.

ISPEPMAX (INTEGER)

Number of iterations for optimizing the a-priori weights.

OUTPUTNAME (CHARACTER\*15)

The name of the output file.

KREL (INTEGER)

Selects the kinematical channels to be used for the phase space generation. KREL=0 is the recommended value for normal runs.

LQED (INTEGER)

It includes (1) or excludes (0) ISR.

LQ\_PT1 (INTEGER)

Collinear QED radiation from the incoming  $e^+$  (0) or generation of ISR photons with non zero  $p_t$  (1).

LQ\_PT2 (INTEGER)

Collinear QED radiation from the incoming  $e^-$  (0) or generation of ISR photons with non zero  $p_t$  (1).

LQ\_SC1 (INTEGER)

$t$ -channel ISR scale for the incoming  $e^+$  off (0) or on (1). When choosing (0), ISR is computed with the scale  $Q^2 = s$ . When choosing (1), if the process has at least 1 final state  $e^+$ , the used scale is  $Q^2 = |t|$ . When there are 2  $e^+$  in the final state, the used scale is  $Q^2 = \min(|t|)$ .

LQ\_SC2 (INTEGER)

$t$ -channel ISR scale for the incoming  $e^-$  as above.

IWIDTH (INTEGER)

Option for the treatment of boson masses and running of  $\alpha_{EM}$ . If IWIDTH=1 all boson masses are taken to be complex, also in the couplings. When IWIDTH=2  $\alpha_{EM}$  is running and the Modified Fermion-Loop is switched on.

IHIGGS (INTEGER)

Higgs diagrams included (1) or not (0).

REL (REAL\*8)

Electron mass.

RNE (REAL\*8)

Mass of  $\nu_e$ .

RMU (REAL\*8)

Muon mass.

RNM (REAL\*8)

Mass of  $\nu_\mu$ .

RTA (REAL\*8)

Tau mass.

RNT (REAL\*8)

Mass of  $\nu_\tau$ .

RUQ (REAL\*8)

Mass of the  $u$  quark.

RDQ (REAL\*8)  
Mass of the  $d$  quark.

RCQ (REAL\*8)  
Mass of the  $c$  quark.

RSQ (REAL\*8)  
Mass of the  $s$  quark.

RTQ (REAL\*8)  
Mass of the  $t$  quark.

RBQ (REAL\*8)  
Mass of the  $b$  quark.

ROOTS (REAL\*8)  
The total energy of the colliding  $e^+$  and  $e^-$ . All energies are in GeV.

SHCUT (REAL\*8)  
Minimum value of the invariant mass squared of the event after ISR.

ECUT(3) (REAL\*8)  
Minimum energy of particle number 3.

ECUT(4) (REAL\*8)  
Minimum energy of particle number 4.

ECUT(5) (REAL\*8)  
Minimum energy of particle number 5.

ECUT(6) (REAL\*8)  
Minimum energy of particle number 6.

SCUT(3,4) (REAL\*8)  
Minimum value of  $(p(3) + p(4))^2$ . All invariant masses in  $\text{GeV}^2$ .

SCUT(3,5) (REAL\*8)

Minimum value of  $(p(3) + p(5))^2$ .

SCUT(3,6) (REAL\*8)

Minimum value of  $(p(3) + p(6))^2$ .

SCUT(4,5) (REAL\*8)

Minimum value of  $(p(4) + p(5))^2$ .

SCUT(4,6) (REAL\*8)

Minimum value of  $(p(4) + p(6))^2$ .

SCUT(5,6) (REAL\*8)

Minimum value of  $(p(5) + p(6))^2$ .

CMAX(1,3) (REAL\*8)

Maximum value of  $\cos \theta$  between particle 1 and 3.

CMAX(1,4) (REAL\*8)

Maximum value of  $\cos \theta$  between particle 1 and 4.

CMAX(1,5) (REAL\*8)

Maximum value of  $\cos \theta$  between particle 1 and 5.

CMAX(1,6) (REAL\*8)

Maximum value of  $\cos \theta$  between particle 1 and 6.

CMAX(2,3) (REAL\*8)

Maximum value of  $\cos \theta$  between particle 2 and 3.

CMAX(2,4) (REAL\*8)

Maximum value of  $\cos \theta$  between particle 2 and 4.

CMAX(2,5) (REAL\*8)

Maximum value of  $\cos \theta$  between particle 2 and 5.

CMAX(2,6) (REAL\*8)

Maximum value of  $\cos \theta$  between particle 2 and 6.

`CMAX(3,4) (REAL*8)`

Maximum value of  $\cos \theta$  between particle 3 and 4.

`CMAX(3,5) (REAL*8)`

Maximum value of  $\cos \theta$  between particle 3 and 5.

`CMAX(3,6) (REAL*8)`

Maximum value of  $\cos \theta$  between particle 3 and 6.

`CMAX(4,5) (REAL*8)`

Maximum value of  $\cos \theta$  between particle 4 and 5.

`CMAX(4,6) (REAL*8)`

Maximum value of  $\cos \theta$  between particle 4 and 6.

`CMAX(5,6) (REAL*8)`

Maximum value of  $\cos \theta$  between particle 5 and 6.

A last remark is in order. When running with the options `LQ_PT1= 1` and `LQ_PT2= 1` for processes with more than one  $e^-$  (or  $e^+$ ) in the final state, even by cutting out the beam cone the generation efficiency of `NEXTCALIBUR` may be bad, due to genuine  $\gamma\gamma$  like events *kicked out* from the beam cone by large  $p_t$  photons. If one is interested just in the total cross section, running with `LQ_PT1 = LQ_PT2= 0` solves the problem, otherwise a reasonable cut on the  $p_t$  of the generated photons must be applied to restore the efficiency.

## 9 Test Run Output

We conclude our description with an example of a calculation that can be performed with `NEXTCALIBUR`. Notice that no cut is present on the final state particles. One should be able to reproduce this output within the estimated Monte Carlo error. Using an input file as follows



```

el          ! par(3)      - produced fermion
ne          ! par(4)      - produced antifermion
uq          ! par(5)      - produced fermion
dq          ! par(6)      - produced antifermion
250000     ! nipt           - number of Monte Carlo points
10000      ! nwarm          - points for the warming
40000      ! nopt           - points for a.p.weights optim
2          ! istepmax       - iterations for a.p.weights optim
output     ! outputname     - program name
0          ! krel   (0:5)  - Channels for MC Mapping
1          ! lqed   (0,1) - QED off or on
0          ! lq_pt1 (0,1) - finite pt for incoming e(+)
0          ! lq_pt2 (0,1) - finite pt for incoming e(-)
1          ! lq_sc1 (0,1) - t-chan scale for incoming e(+)
1          ! lq_sc2 (0,1) - t-chan scale for incoming e(-)
2          ! iwidth (1:2) - option for boson masses and running
0          ! ihiggs (0:1) - Higgs included or not
0.51099906d-3 ! rel          - fermion masses:
0.d0        ! rne          -
105.658389d-3 ! rmu         -
0.d0        ! rnm         -
1.77705d0   ! rta         -
0.d0        ! rnt         - be aware that when
0.005d0     ! ruq         - fermion masses are zero
0.010d0     ! rdq         - the computation gets faster!
1.55d0      ! rcq         -
150.d-3     ! rsq         -
175.d0      ! rtq         -
4.7d0       ! rbq         -
200.d0      ! roots       - center of mass energy (GeV)
0.d0        ! shcut       - cut on inv. mass squared after QED
0.d0        ! ecut_3      - Energy cut for particle 3
0.d0        ! ecut_4      - Energy cut for particle 4
0.d0        ! ecut_5      - Energy cut for particle 5
0.d0        ! ecut_6      - Energy cut for particle 6
0.d0        ! scut_34     - inv. mass cut for the system (34)
0.d0        ! scut_35     - inv. mass cut for the system (35)

```

```

0.d0          ! scut_36      - inv. mass cut for the system (36)
0.d0          ! scut_45      - inv. mass cut for the system (45)
0.d0          ! scut_46      - inv. mass cut for the system (46)
0.d0          ! scut_56      - inv. mass cut for the system (56)
1.d0          ! cmax_13      - cut on cos_(1,3)
1.d0          ! cmax_14      - cut on cos_(1,4)
1.d0          ! cmax_15      - cut on cos_(1,5)
1.d0          ! cmax_16      - cut on cos_(1,6)
1.d0          ! cmax_23      - cut on cos_(2,3)
1.d0          ! cmax_24      - cut on cos_(2,4)
1.d0          ! cmax_25      - cut on cos_(2,5)
1.d0          ! cmax_26      - cut on cos_(2,6)
1.d0          ! cmax_34      - cut on cos_(3,4)
1.d0          ! cmax_35      - cut on cos_(3,5)
1.d0          ! cmax_36      - cut on cos_(3,6)
1.d0          ! cmax_45      - cut on cos_(4,5)
1.d0          ! cmax_46      - cut on cos_(4,6)
1.d0          ! cmax_56      - cut on cos_(5,6)

```

and the input values

$$\begin{aligned}
G_F &= 1.6637 \cdot 10^{-5} \text{ GeV}^{-2} & M_Z &= 91.1867 \text{ GeV} \\
M_W &= 80.35 \text{ GeV} & \Gamma_Z &= 2.4939 \text{ GeV} \\
\Gamma_W &= \frac{3G_F M_W^2}{\pi\sqrt{8}} & \sin^2 \theta_W &= 1 - \frac{M_W^2}{M_Z^2} \\
\alpha &= \sin_W^2 G_F M_W^2 \frac{\sqrt{2}}{\pi},
\end{aligned}$$

we get the following output file

output

```
process :   antiel(1) el(2) ----> el(3) antine(4) uq(5) antidq(6)
```

This run is with:

```

nipt      =      250000
nwarm     =      10000

```

```
nopt      =      40000
istepmax=      2
krel      =      0
lqed      =      1
lq_pt1    =      0
lq_pt2    =      0
lq_sc1    =      1
lq_sc2    =      1
iwidth    =      2
ihiggs    =      0
rel        =      0.510999D-03
rne        =      0.000000D+00
rmu        =      0.105658D+00
rnm        =      0.000000D+00
rta        =      0.177705D+01
rnt        =      0.000000D+00
ruq        =      0.500000D-02
rdq        =      0.100000D-01
rcq        =      0.155000D+01
rsq        =      0.150000D+00
rtq        =      0.175000D+03
rbq        =      0.470000D+01
roots      =      0.200000D+03
shcut      =      0.000000D+00
ecut_3     =      0.000000D+00
ecut_4     =      0.000000D+00
ecut_5     =      0.000000D+00
ecut_6     =      0.000000D+00
scut_34    =      0.000000D+00
scut_35    =      0.000000D+00
scut_36    =      0.000000D+00
scut_45    =      0.000000D+00
scut_46    =      0.000000D+00
scut_56    =      0.000000D+00
cmax_13    =      0.100000D+01
cmax_14    =      0.100000D+01
cmax_15    =      0.100000D+01
```

```

cmax_16 = 0.100000D+01
cmax_23 = 0.100000D+01
cmax_24 = 0.100000D+01
cmax_25 = 0.100000D+01
cmax_26 = 0.100000D+01
cmax_34 = 0.100000D+01
cmax_35 = 0.100000D+01
cmax_36 = 0.100000D+01
cmax_45 = 0.100000D+01
cmax_46 = 0.100000D+01
cmax_56 = 0.100000D+01

```

Input parameters:

```

gfermi = 0.116637D-04
zm      = 0.911867D+02
wm      = 0.803500D+02
zw      = 0.249390D+01
ww      = 0.204277D+01
sin2w   = 0.223558D+00
1/alpha = 0.131958D+03
hm      = 0.120000D+03
hw      = 0.236865D-02

```

-----

Kinematical Diagrams:

| channel           | permutation |
|-------------------|-------------|
| 1: annihi2(wm)    | 1 2 3 4 5 6 |
| 2: annihi2(wm)    | 1 2 4 3 5 6 |
| 3: annihi2(wm)    | 1 2 5 6 3 4 |
| 4: annihi2(wm)    | 1 2 6 5 3 4 |
| 5: bremf4(wm)     | 1 2 3 4 5 6 |
| 6: bremb2(wm)     | 2 1 3 4 5 6 |
| 7: conver3(wm,wm) | 1 2 5 6 3 4 |

```

8: multi2          2 1 3 5 6 4
9: multi3          1 2 3 5 6 4
10: nonab1(wm)     1 2 3 4 5 6
11: nonab2(wm)     2 1 3 5 6 4
12: nonab4(wm)     1 2 3 5 6 4
13: rambo4         1 2 3 4 5 6

```

-----

Differences in the computation  
of the a-priori weights:

```

diff(      1 )= 5.38443233306179
diff(      2 )= 6.18288649090395
diff(      3 )= 2.25190931218116

```

a-priori weights:

```

1 : 0.301826D-01
2 : 0.202852D-01
3 : 0.210927D-01
4 : 0.327752D-01
5 : 0.251601D-01
6 : 0.873505D-01
7 : 0.299054D+00
8 : 0.185762D+00
9 : 0.199223D-02
10 : 0.162069D+00
11 : 0.104346D+00
12 : 0.251601D-01
13 : 0.477138D-02

```

-----

Cross Section (pb):

```

1 0.79733D+00 +/- 0.46D-02

```

## A The kinematical channel MULTI1

We refer to fig. 1 and split the integration over the massive four-body phase space into a 3-body decay times a 2-body decay

$$\int d(P S)_4 = \int ds_{45} I_3(p_3, p_6, p_{45}) I_2(p_4, p_5), \quad (30)$$

with

$$\begin{aligned} I_3(p_3, p_6, p_{45}) &= \int D(p_3, m_3^2) D(p_6, m_6^2) D(p_{45}, s_{45}) \delta^4(p_{12} - p_3 - p_6 - p_{45}), \\ I_2(p_4, p_5) &= \int D(p_4, m_4^2) D(p_5, m_5^2) \delta^4(p_{45} - p_4 - p_5), \\ D(p_i, m_i^2) &= d^4 p_i \delta(p_i^2 - m_i^2) \theta(E_i), \quad p_{ij} = p_i + p_j, \quad s_{45} = p_{45}^2. \end{aligned} \quad (31)$$

The three-body phase space can be rewritten as

$$I_3(p_3, p_6, p_{45}) = \frac{s}{32} \int_{2\sqrt{\mu_3}}^{x_-} dx \int dy d\Omega_3 d\Omega_6 \delta[F(x, y)], \quad (32)$$

where  $x$  and  $y$  are the reduced energies of the particles 3 and 6

$$E_3 = \frac{\sqrt{s}}{2} x, \quad E_6 = \frac{\sqrt{s}}{2} y,$$

$d\Omega_i = d\phi_i d\cos\theta_i$  is the integration element over the solid angle of particle  $i$  and  $c_{36}$  the cosine of the angle between particles 3 and 6. Finally,

$$\begin{aligned} F(x, y) &= 2G(x, y)/\sqrt{H(x, y)} - c_{36}, \quad G(x, y) = M - x - y + \frac{xy}{2}, \\ H(x, y) &= (x^2 - 4\mu_3)(y^2 - 4\mu_6), \quad M = 1 + \mu_3 + \mu_6 - \mu, \\ \mu_i &= \frac{m_i^2}{s}, \quad \mu = \frac{s_{45}}{s}, \quad x_- = (1 + \mu_3) - (\sqrt{\mu} + \sqrt{\mu_6})^2. \end{aligned} \quad (33)$$

Eq. (32) is equivalent to

$$\begin{aligned} I_3(p_3, p_6, p_{45}) &= \\ &= \frac{s}{32} \int_{2\sqrt{\mu_3}}^{x_-} dx \int dy d\Omega_3 d\Omega_6 \frac{1}{|F'(x, y)|} [\delta(y - y_+) + \delta(y - y_-)], \end{aligned} \quad (34)$$

where

$$\begin{aligned}
F'(x, y) &= \frac{\partial F(x, y)}{\partial y}, \quad y^\pm = \frac{\beta \pm \sqrt{\Delta}}{\alpha}, \quad \Delta = \beta^2 - \alpha\gamma, \\
\alpha &= 4 \left(1 - \frac{x}{2}\right)^2 - c_{36}^2 (x^2 - 4\mu_3), \quad \beta = 4 \left(1 - \frac{x}{2}\right) (M - x), \\
\gamma &= 4(M - x)^2 + 4c_{36}^2 \mu_6 (x^2 - 4\mu_3).
\end{aligned} \tag{35}$$

As for the two-body decay, the following expression holds

$$\begin{aligned}
I_2(p_4, p_5) &= \frac{1}{8s_{45}} \lambda(s_{45}, m_4^2, m_5^2) \int d\Omega_4, \\
\lambda(a, b, c) &= \sqrt{a^2 + b^2 + c^2 - 2ab - 2ac - 2bc}.
\end{aligned} \tag{36}$$

The first four steps of the generation algorithm are as follows:

1) generate  $s_{45}$  with distribution

$$\frac{1}{s_{45}};$$

2) generate  $x$  with distribution

$$\frac{1}{1-x};$$

3) generate  $\phi_3$  uniformly and  $c_3 \equiv \cos \theta_3$  with distribution

$$\frac{1}{a_3 - c_3}, \quad a_3 = \frac{E_1 E_3 - m_e^2}{|\vec{p}_1| |\vec{p}_3|};$$

4) generate  $\phi_6$  uniformly and  $c_6 \equiv \cos \theta_6$  with distribution

$$\frac{1}{a_6 - c_6}, \quad a_6 = \frac{E_2 \tilde{E}_6 - m_e^2}{|\vec{p}_2| |\vec{p}_6|}, \quad \tilde{E}_6 = \frac{\sqrt{s}}{2} \tilde{y}, \quad |\vec{p}_6| = \sqrt{\tilde{E}_6^2 - m_e^2}, \tag{37}$$

where  $\tilde{y}$  is the solution of the equation

$$2G(x, \tilde{y}) / \sqrt{H(x, \tilde{y})} + 1 = 0. \tag{38}$$

The reason for the above choice of  $a_6$  is that, at this stage of generation,  $E_6$  is unknown, but its value when  $c_{36} = -1$  (namely when the multiperipheral singularity is more pronounced) can be computed using the condition  $F(x, \tilde{y}) = 0$ , as read from eq. (33) with  $c_{36} = -1$ .

From the generated values of  $c_3$ ,  $c_6$ ,  $\phi_3$  and  $\phi_6$  one then computes

$$c_{36} = \cos \theta_3 \cos \theta_6 + \sin \theta_3 \sin \theta_6 \cos(\phi_3 - \phi_6),$$

to be compared with two possible values ( $c_{36}^\pm$ ) obtained from the conditions  $y = y^\pm$  in eq. (34). There are four possibilities. If  $c_{36} \neq c_{36}^\pm$  the event has vanishing weight. If  $c_{36} = c_{36}^+ \neq c_{36}^-$ , then  $y = y^+$  and only the first term in eq. (34) contributes. If  $c_{36} = c_{36}^- \neq c_{36}^+$ , then the second term in eq. (34) has to be chosen. Finally, if  $c_{36} = c_{36}^+ = c_{36}^-$ , the two terms are picked up randomly and the total event weight multiplied by 2.

The last part of the generation accounts for the  $t$ -channel exchanged fermion in MULTI1. By defining  $q = p_1 - p_3$ , the variable  $c_4 \equiv \cos \theta_4$  peaks, in the rest frame of  $s_{45}$ , as follows

$$\frac{1}{a - c_4}, \quad a = \frac{2q_0 E_4 - q^2}{2|\vec{q}||\vec{p}_4|}, \quad E_4 = \frac{s_{45} + m_4^2 - m_5^2}{2\sqrt{s_{45}}}. \quad (39)$$

On the other hand, also the diagram obtained when replacing  $p_4 \leftrightarrow p_5$  contributes with an analogous peaking behaviour

$$\frac{1}{b - c_5}, \quad b = \frac{2q_0 E_5 - q^2}{2|\vec{q}||\vec{p}_5|}, \quad E_5 = \frac{s_{45} + m_5^2 - m_4^2}{2\sqrt{s_{45}}}. \quad (40)$$

Since, in the rest frame of  $s_{45}$ ,  $c_4 = -c_5$ , both distributions can be simultaneously mapped, via the last three items of our generation algorithm:

- 5) go the rest frame of  $s_{45}$ ;
- 6) generate  $\phi_4$  uniformly and  $c_4$  with distribution

$$\frac{1}{(a - c_4)(b + c_4)};$$

- 7) boost  $p_4$  and  $p_5$  back to the lab frame.



A massive four-fermion event is then generated, taking into account all peaks due to  $t$ -channel exchanged massless or nearly massless particles.

In NEXTCALIBUR the described procedure is further refined by making it fully symmetric under the replacements  $\{p_1, p_3\} \leftrightarrow \{p_2, p_6\}$ .

Finally, the same ingredients are used also when constructing the channel MULTI2, the only variation being a different choice of the distributions employed in the generation of some of the variables.

## B The Modified Fermion-Loop approach

Following ref. [16] we split the bare W and Z boson self-energies into universal and non universal contributions

$$\begin{aligned}\hat{\Sigma}_W(p^2) &= \hat{\Sigma}_W(p^2) + \hat{g}^2 T_W(p^2), \\ \hat{\Sigma}_Z(p^2) &= \hat{\Sigma}_Z(p^2) + \frac{\hat{g}^2}{\hat{c}^2} T_Z(p^2),\end{aligned}\quad (41)$$

where  $\hat{g}$  is the bare weak coupling constant  $\hat{s}$  the sine of the bare mixing angle and  $\hat{c}^2 \equiv 1 - \hat{s}^2$ . When including fermion loops only, the explicit expressions for the above quantities are

$$\begin{aligned}\hat{\Sigma}_W(p^2) &= \frac{\hat{g}^2}{48\pi^2} \frac{1}{2} \sum_f N_f^c \left\{ I(p^2) + (1 + 2I_{3f} Y_f) F(p^2, m_f) \right\}, \\ \hat{\Sigma}_Z(p^2) &= \frac{\hat{g}^2}{48\hat{c}^2\pi^2} \sum_f N_f^c \left\{ (\hat{v}_f^2 + \hat{a}_f^2) I(p^2) \right. \\ &\quad \left. + (\hat{v}_f^2 + \hat{a}_f^2 + 4I_{3f} Y_f \hat{a}_f^2) F(p^2, m_f) \right\},\end{aligned}\quad (42)$$

with  $Y_f = 2(Q_f - I_{3f})$ ,  $v_f = I_{3f} - 2\hat{s}^2 Q_f$ ,  $a_f = -I_{3f}$  and  $N_f^c =$  number of colors. Furthermore

$$\begin{aligned}I(p^2) &= -p^2 f(\epsilon) \left[ \frac{2}{\epsilon} + \ln(-p^2) - \frac{5}{3} \right], \\ F(p^2, m) &= -6p^2 f(\epsilon) G(p^2, p^2, m), \\ G(s, t, m) &= \int_0^1 dx \left\{ x(1-x) \ln \frac{m^2 - sx(1-x)}{-tx(1-x)} \right\}, \\ f(\epsilon) &= \pi^{\frac{\epsilon}{2}} \Gamma\left(1 - \frac{\epsilon}{2}\right), \quad \text{with } \epsilon = n_d - 4.\end{aligned}\quad (43)$$

Finally, the leading contribution to  $T_{W,Z}(p^2)$  originate from the top quark:

$$\begin{aligned}
T_W(p^2) &= f(\epsilon) \frac{3}{16\pi^2} \left\{ m_t^2 \left[ \frac{1}{\epsilon} + \frac{1}{2} \ln m_t^2 - \frac{1}{4} + J_0(b) - J_1(b) \right] \right. \\
&\quad \left. - 2p^2 \left[ J_1(b) - J_2(b) + \frac{5}{36} - \frac{1}{6} \ln(b) - \frac{2}{3} G(p^2, p^2, m_t) \right] \right\}, \\
T_Z(p^2) &= f(\epsilon) \frac{1}{16\pi^2} \left\{ \frac{3}{2} m_t^2 \left[ \frac{2}{\epsilon} + \ln m_t^2 + J_0(b_+) + J_0(b_-) \right] \right. \\
&\quad \left. + p^2 G(p^2, p^2, m_t) \right\}, \tag{44}
\end{aligned}$$

where

$$J_i(b) = \int_0^1 dx x^i \ln(1+bx), \quad b = -\frac{p^2}{m_t^2}, \quad b_{\pm} = \frac{1}{x_{\pm}}, \quad x_{\pm}^2 - x_{\pm} + \frac{1}{b} = 0. \tag{45}$$

Two more expressions are necessary, namely the photon ( $\hat{\Sigma}_\gamma$ ) and the photon-Z mixing ( $\hat{\Sigma}_X$ ) self-energies

$$\hat{\Sigma}_\gamma(p^2) = \frac{\hat{g}^2 \hat{s}^2}{12\pi^2} \sum_f Q_f^2 N_f^c \left\{ I(p^2) + F(p^2, m_f) \right\}, \tag{46}$$

$$\hat{\Sigma}_X(p^2) = -\frac{\hat{g}^2}{24\pi^2} \frac{\hat{s}}{\hat{c}} \sum_f \hat{v}_f Q_f N_f^c \left\{ I(p^2) + F(p^2, m_f) \right\}. \tag{47}$$

In terms of self-energies the running couplings are defined as follows

$$\frac{e^2(p^2)}{\hat{g}^2 \hat{s}^2} = \frac{p^2}{p^2 + \hat{\Sigma}_\gamma(p^2)}, \quad \frac{g^2(p^2)}{\hat{g}^2} = \frac{p^2}{p^2 + \hat{\Sigma}_W(p^2)}, \quad s^2(p^2) = \frac{e^2(p^2)}{g^2(p^2)}. \tag{48}$$

Since, as explained in section 5, we are only interested in the real part of the corrections, we renormalize the W and Z boson propagators at the real mass

$$\begin{aligned}
M_W^2 &= \hat{\mu}_w - \text{Re} \hat{\Sigma}_W(M_W^2), \\
M_Z^2 &= \hat{\mu}_z - \text{Re} \hat{Z}(M_W^2), \tag{49}
\end{aligned}$$

where  $\hat{\mu}_{w,z}$  are the bare gauge boson masses squared and

$$\hat{Z}(p^2) = \hat{\Sigma}_Z(p^2) - \frac{\hat{\Sigma}_X^2(p^2)}{p^2 + \hat{\Sigma}_\gamma(p^2)}. \tag{50}$$

Finally,  $G_F$  fixes our third fitting equation

$$\frac{G_F}{\sqrt{2}} = \frac{\hat{g}^2}{8(\hat{\mu}_W - \hat{\Sigma}_W(0))}. \quad (51)$$

By solving the above equations it is easy to get  $\hat{g}^2$ ,  $\hat{\mu}_w$  and  $\hat{s}^2$  in terms of  $G_F$ ,  $M_W^2$  and  $M_Z^2$ . Putting everything together, the running couplings read

$$\begin{aligned} g^2(s) = & M_W^2 a \operatorname{Re} \left\{ 1 + \frac{3}{2} M_W^2 \frac{a}{\pi^2} G(M_W^2, s, 0) - \frac{M_W^2 a}{8\pi^2} [G(s, s, m_e) \right. \\ & + G(s, s, m_\mu) + G(s, s, m_\tau) + 2G(s, s, m_u) + 2G(s, s, m_c) \\ & + 2G(s, s, m_t) - 2G(M_W^2, M_W^2, m_t) + G(s, s, m_d) \\ & \left. + G(s, s, m_s) + G(s, s, m_b)] - a [T_W(M_W^2) - T_W(0)] \right\}^{-1}, \quad (52) \end{aligned}$$

and

$$\begin{aligned} e^2(s) = & M_W^2 a N \operatorname{Re} \left\{ \left[ 1 - a [T_W(M_W^2) - T_W(0)] + \frac{3}{2} \frac{M_W^2 a}{\pi^2} G(M_W^2, M_Z^2, 0) \right. \right. \\ & \left. \left. + \frac{1}{4} \frac{M_W^2 a}{\pi^2} (G(M_W^2, M_W^2, m_t) - G(M_Z^2, M_Z^2, m_t)) \right]^2 \right. \\ & - \frac{4}{\pi^2} M_W^2 a N \left[ G(s, M_Z^2, 0) + \frac{1}{8} [G(s, s, m_e) + G(s, s, m_\mu) \right. \\ & \left. + G(s, s, m_\tau)] + \frac{1}{6} [G(s, s, m_u) + G(s, s, m_c) + G(s, s, m_t)] \right. \\ & \left. - \frac{1}{6} G(M_Z^2, M_Z^2, m_t) + \frac{1}{24} [G(s, s, m_d) + G(s, s, m_s)] \right. \\ & \left. \left. + \frac{1}{24} G(s, s, m_b) \right] \right\}^{-1}, \quad (53) \end{aligned}$$

where

$$\begin{aligned} N = & 1 - \frac{M_W^2}{M_Z^2} \left[ 1 - a \operatorname{Re}(T_Z(M_Z^2) - T_W(0)) \right] \\ & - a \operatorname{Re}(T_W(M_W^2) - T_W(0)) + \frac{3}{2} \frac{M_W^2 a}{\pi^2} G(M_W^2, M_Z^2, 0) \end{aligned}$$

$$\begin{aligned}
& + \frac{1}{4} \frac{M_W^2 a}{\pi^2} \operatorname{Re} \left[ G(M_W^2, M_W^2, m_t) - G(M_Z^2, M_Z^2, m_t) \right], \\
a & = \frac{8G_F}{\sqrt{2}}. \tag{54}
\end{aligned}$$

A comment is in order on the appearance of the light quark masses in the above expressions. The weak coupling  $g^2(s)$  gives sizable contributions at high energies, where all light fermion masses can be neglected, so that only the top terms survive in eq. (52). On the contrary, being interested in the low energy regime of eq. (53), we have to include in our formulae the hadron vacuum polarization  $\Delta_r^h(s)$ , as computed in ref. [20], rather than using quark masses. By inserting

$$\begin{aligned}
\operatorname{Re} G(s, s, m) & = \frac{1}{6} \ln \frac{m^2}{|s|} + \frac{5}{18} + \operatorname{Re} J(s, m), \\
J(s, m) & = \int_0^1 dx x(1-x) \ln \left( 1 - \frac{s}{m^2} x(1-x) \right) \tag{55}
\end{aligned}$$

in eq. (53), one gets

$$\begin{aligned}
e^2(s) & = M_W^2 a N \operatorname{Re} \left\{ \left[ 1 - a [T_W(M_W^2) - T_W(0)] + \frac{3}{2} \frac{M_W^2 a}{\pi^2} G(M_W^2, M_Z^2, 0) \right. \right. \\
& + \left. \left. \frac{1}{4} \frac{M_W^2 a}{\pi^2} \left( G(M_W^2, M_W^2, m_t) - G(M_Z^2, M_Z^2, m_t) \right) \right]^2 \right. \\
& + \frac{2}{3\pi^2} M_W^2 a N \left[ J(M_Z^2, m_t) - J(s, m_t) \right] \\
& - \frac{4}{\pi^2} M_W^2 a N \left[ \frac{25}{108} + \frac{1}{48} \sum_{\ell=e,\mu,\tau} \ln \frac{m_\ell^2}{M_Z^2} + \frac{1}{36} \sum_{q=u,c} \ln \frac{m_q^2}{M_Z^2} \right. \\
& \left. \left. + \frac{1}{144} \sum_{q=d,s,b} \ln \frac{m_q^2}{M_Z^2} + \frac{1}{8} \sum_{\ell=e,\mu,\tau} J(s, m_\ell) + \frac{\pi}{16\alpha(0)} \Delta_r^h(s) \right] \right\}^{-1}, \tag{56}
\end{aligned}$$

with  $1/\alpha(0) = 137.0359895$ . Notice that, due to our choice of the input parameter set, a dependence on the light quark masses is left in the previous equation. However, since the pure bosonic corrections are missing,  $m_t$  can be interpreted as a free parameter [16] to be fitted in such a way that  $\alpha(0) \equiv$

$e^2(0)/4\pi = 1/137.0359895$ . The quark masses appearing in eq. (56) only affect this fitting procedure, and not the running of the electro-magnetic coupling. In other words, a change in the  $m_q$ 's is compensated by a different fitted value for  $m_t$ . For consistency, in **NEXTCALIBUR** the light quark masses are taken to be those that reproduce the hadronic vacuum polarization, but the numerical results are rather insensitive to the initial choice of  $m_q$ 's.

Eqs. (52) and (56), together with equations (25)-(28) completely define our Modified Fermion-Loop approach.

## Acknowledgements

Discussions with the participants in the CERN LEP2 Monte Carlo Workshop [2] are acknowledged. The authors also acknowledge the financial support of the European Union under contract HPRN-CT-2000-00149.

## References

- [1] D. Bardin et al., in *Physics at LEP2*, CERN 96-01 (1996), eds. G. Altarelli, T. Sjöstrand and F. Zwirner, Vol 2, p. 3.
- [2] M. W. Grünewald et al., in *Reports of the working groups on precision calculations for LEP2 Physics*, CERN 2000-009 (2000), eds. S. Jadach, G. Passarino and R. Pittau, p. 1, hep-ph/0005309.
- [3] F. A. Berends, R. Pittau and R. Kleiss, *Comput. Phys. Commun.* **85**, 437 (1995) and *Nucl. Phys.* **B424**, 308 (1994).
- [4] F. A. Berends, C. G. Papadopoulos and R. Pittau, hep-ph/0002249 and ref. [2], sections 5.1 and 6.2.
- [5] A. Kanaki and C. G. Papadopoulos, hep-ph/0002082.
- [6] R. Kleiss and R. Pittau, *Comput. Phys. Commun.* **83** (1994) 141.
- [7] E. A. Kuraev and V. S. Fadin, *Yad. Fiz.* **41**, 753 (1985) [*Sov. J. Nucl. Phys.* **41**, 466 (1985)];  
G. Altarelli and G. Martinelli, in *Physics at LEP*, CERN-Yellow Report

- 86-06, eds. J. Ellis and R. Peccei (CERN, Geneva, February 1986);  
O. Nicrosini and L. Trentadue, Phys. Lett. **B196**, 551 (1987);  
F. A. Berends, G. Burgers and W. L. van Neerven, Nucl. Phys. **B297**,  
429 (1988) and **B304**, 921E (1988).
- [8] G. Montagna, M. Moretti, O. Nicrosini and F. Piccinini, Nucl. Phys.  
**B541**, 31 (1999);  
O. Nicrosini and L. Trentadue, Nucl. Phys. **B318**, 1 (1989) and Phys.  
Lett. **B231**, 487 (1989).
- [9] F. A. Berends and R. Kleiss, Nucl. Phys. **B260**, 32 (1985) and **B178**,  
141 (1981).
- [10] W. Beenakker, F. A. Berends and S. C. van der Marck, Nucl. Phys.  
**B349**, 323 (1991).
- [11] Y. Kurihara, J. Fujimoto, Y. Shimizu, K. Kato, K. Tobimatsu and  
T. Munehisa, Prog. Theor. Phys. **103**, 1199 (2000).
- [12] F. A. Berends, P. H. Daverveldt and R. Kleiss, Nucl. Phys. **B253**, 421  
(1985).
- [13] G. Montagna, M. Moretti, O. Nicrosini, A. Pallavicini and F. Piccinini,  
hep-ph/0005121
- [14] S. Jadach, W. Placzek, M. Skrzypek and B. F. L. Ward, Phys. Rev.  
**D54**, 5434 (1996).
- [15] G. Passarino, Nucl. Phys. **B574**, 451 (2000) and **B578**, 3 (2000).
- [16] W. Beenakker et al., Nucl. Phys. **B500**, 255 (1997).
- [17] E. Argyres et al., Phys. Lett. **B358**, 339 (1995).
- [18] See the contribution by WPHACT to ref. [2], and E. Accomando,  
A. Ballestrero and E. Maina, Phys. Lett. **B479**, 209 (2000)
- [19] W. Beenakker, F. A. Berends and A. P. Chapovsky, Nucl. Phys. **B573**,  
503 (2000).
- [20] S. Eidelman and F. Jegerlehner, Z. Phys. **C67** (1995) 585.